

## ***The Mechanics of Laminated Rubber Bearings***

T J POND\* AND A G THOMAS\*

*A study of the behaviour of laminated rubber bearings is described with particular emphasis on important aspects concerned with seismic isolation. Theory with supporting experimental data are given which describe the effect of compressive load on damping and the height reduction behaviour of a bearing under combined compression and shear. A study of shear stiffness and the tilting of individual rubber layers in a bearing is also described, and indicates that a departure from the normal linear shear stiffness behaviour occurs at large deformations, and that cavitation is responsible*

Laminated rubber bearings are used in a variety of applications requiring vibration isolation. During the last decade, they have been increasingly used as building mounts to protect buildings from earthquake damage. In many respects this is a more demanding application than those in which the vibrations to be isolated are due to mechanical origins as these are usually of relatively small amplitude. Earthquake bearings may typically have to sustain horizontal displacements of some hundreds or millimetres without failure. Other important design considerations are: i) the vertical stiffness must be sufficiently great to prevent rocking of the building and to avoid resonance, ii) the horizontal stiffness has to be sufficiently low to give a horizontal natural frequency of typically 0.5 Hz, iii) the damping during horizontal movements has to be sufficiently great to restrict the maximum values of shear displacement of the bearing and building acceleration experienced during an earthquake to acceptable values.

Some important factors influencing these requirements were previously studied both theoretically and experimentally<sup>1</sup>. This paper describes the experimental procedures employed in conducting this study in greater detail, and also includes extra data on important mechanical aspects associated with the deformation of a bearing. In addition, a further investigation of cavitation failure and

its effect on the shear stiffness of a bearing is described.

### EXPERIMENTAL

To verify the accuracy of the theories given for the effect of mechanical damping and reduction in height on shearing of a bearing, and to study additional important bearing characteristics, the following two separate experimental techniques were employed.

#### **Model Bearing in Free Oscillation**

Experiments have been carried out using small bearings each consisting of ten rectangular rubber layers (dimensions 66.8 × 54 × 3.18 mm) separated by 6.35 mm thick metal plates. The metal reinforcing plates were of sufficient thickness to prevent any bending under the imposed deformations. These bearings are identical to those described previously<sup>1</sup>.

The bearings were constructed by individually hot moulding a layer of natural rubber bonded between two mild steel plates using a proprietary adhesive system (Chemlok 205/220)<sup>2</sup>. Ten such sandwich units were bonded together with epoxy adhesive in a suitable jig to form the complete bearing. This construction technique ensured good reproducibility between layers, particularly with regard to the rubber thickness, which

\* Malaysian Rubber Producers' Research Association, Brickendonbury, Hertford SG13 8NL, United Kingdom

is important in this study to provide good experimental precision for comparison with the theory. The technique was found to give superior layer reproducibility than the more conventional construction method of assembling an entire bearing in a mould before vulcanisation.

A conventional sulphur cured NR vulcanisate containing no carbon black filler was used to construct each bearing. The rubber formulation is given in *Table 1*. The formulation provides adequate physical properties to withstand the normal imposed test deformations without failure, while avoiding the additional complication of a non-linear force-deformation behaviour associated with carbon filled compounds. The formulation also minimises the amount of time-dependent creep and permanent set present. This is particularly important in the static tests described below, where these effects, if large, may significantly reduce the measurement accuracy of the shear displacement of a bearing under a compressive load.

TABLE 1 FORMULATION AND PHYSICAL PROPERTIES

Formulation	Pphr
Natural rubber (SMR 5)	100
Zinc oxide	5
Stearic acid	2
Sulphur	2.5
CBS	0.6
ZA	1.5
Cure 40 min at (140°C)	
Physical property	
Shear modulus	0.50 MPa
Hardness (IRHD)	44

The experiments were designed to test the dependence of horizontal stiffness and damping on normal load predicted by *Equations A1* and *A7* given in the *Appendix* (Thomas<sup>1</sup> gives fuller details). The method was to support on four bearings a load of up to 4000 kg consisting of a series of concrete blocks of known weight.

The four bearings were placed in a square configuration on a levelled concrete floor and the rectangular concrete weights placed carefully on the bearings, using a fork lift truck, ensuring they sat squarely over the configuration. Because of the small amount of damping present in unfilled natural rubber, a non-contacting displacement transducer was found to be essential to measure the logarithmic decrement of the free oscillations and a capacitance type proximity transducer was used. The system was put into motion by a push and successive oscillations were recorded on a chart recorder.

The spacing of each bearing in relation to the concrete blocks proved important since this can influence the natural frequency of torsional oscillation. For measurement purposes, the configuration was arranged so that the natural frequencies of translation and torsion were dissimilar, this ensured that the system oscillated only in one (x) direction. Dissimilar frequencies were achieved by placing the bearings near the corners of the rectangular block. If the natural frequencies were similar in both translation and torsion, which could occur if the bearings were placed symmetrically near the centre of the blocks, coupled oscillations would take place with beating between translational and torsional modes<sup>2</sup>.

In order to improve the accuracy of the experimental data described previously<sup>1</sup>, further measurements have been made of the horizontal stiffness and damping behaviour of a bearing.

With the small amount of damping present in these experiments under small compressive loads, air damping may have contributed to a significant proportion of the damping observed, and some separate measurements were conducted to quantify this effect. Lightweight air vanes of known vertical face area were attached to the concrete blocks and the damping compared to blocks without the vanes. The difference in the damping indicated the magnitude of damping per unit vertical face area, at a given frequency and amplitude, and this figure was used to estimate the

damping contribution of each block. It was found that the oscillating concrete blocks produced small but measurable damping which was allowed for in the damping results given.

### Experiments with Static Model Bearings

*The quadruple shear test apparatus.* In service, earthquake bearings are subjected to simultaneous compression and shear forces, whereas for testing purposes it is difficult to apply these forces simultaneously on a single bearing. Two bearings can be stacked one above the other and the shear force applied at mid-height. This method, however, has two disadvantages. The first is that application of a force on only one side of the stack produces an unbalanced sideways force and transmits bending moments to the test machine. This leads to uncertainties in the measurements of compressive force and possible damage to the machine. The second disadvantage is that the mid-point of the stack, where the shear

force is applied, moves down as the bearing is compressed. A single stack system must, therefore, be articulated to accommodate such movement, which greatly complicates the design. To overcome these problems a quadruple shear apparatus was built, which comprises two stacks of bearings, placed parallel to one another<sup>1</sup>. The apparatus is shown in *Figure 1*. The advantage of the quadruple configuration, where the bearings are forced apart from the centre, is that the two stacks of bearings act against each other so that there is no net sideways force, and thus no bending movements are transmitted to the test machinery. The shear force was applied by a screw thread (a hydraulic system could also be used) *via* a transducer for recording the force. This screw device is only connected to the bearings, so that changes in height during compression do not affect them in any way.

Experiments to measure height reduction under shear were carried out on model bearings similar to those described previously.

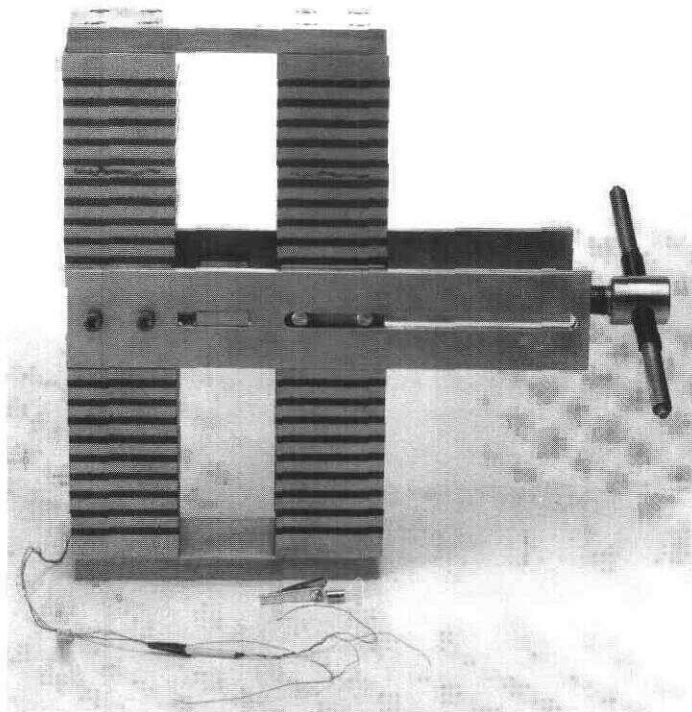


*Figure 1. The quadruple bearing test apparatus.*

The height reduction experiments were conducted by initially applying a known compressive load to the quadruple shear apparatus. The bearings were now forced apart at the centre by rotating the screw thread to the required shear displacement. The compressive load, which reduces when applying the shear force, was adjusted back to the original value and the change in height recorded.

## RESULTS

### Model Bearings in Free Oscillation

From measurements of the free oscillation frequency  $f$  of the loaded bearings with supported mass  $m$ , consisting of the concrete blocks, the stiffness  $K$  of a single bearing was calculated by the relation

$$K = \pi^2 f^2 m \quad 1$$

The experimental results showing the variation of shear stiffness with compressive load for a single bearing are shown in Figure 2. A theoretical curve derived from Equation A1

is also shown, the values  $T$  (44 kNm<sup>2</sup>) and  $R$  (4.3 kN), the tilting and shear stiffness per unit height, being chosen to give the best fit. The additional experimental data presented here has enabled a closer curve fit than that given previously<sup>1</sup>, which provides better agreement between the theoretical values of  $T$  and  $R$  and the experimental results. The values of  $T$  and  $R$  are related to the shear modulus of the rubber and the bearing dimensions by Equations A2 and A3 for circular bearings. Equation A2 still applies for the present rectangular cross section, and the experimentally observed value of  $R$  (4.3 kN) is consistent with a  $G$  value of 0.5 MPa which is consistent with the known modulus (0.5 MPa) of this compound<sup>6</sup>. The  $T$  value for a rectangular bearing is given by Gent and Meinecke<sup>7</sup>. Using their theory and the present dimensions,  $T/R$  (which is independent of  $G$ ) is calculated to be  $1.11 \times 10^{-2}$  square metre, which corresponds well with the experimental value of  $1.02 \times 10^{-2}$  square metre. The experimentally determined damping is shown in

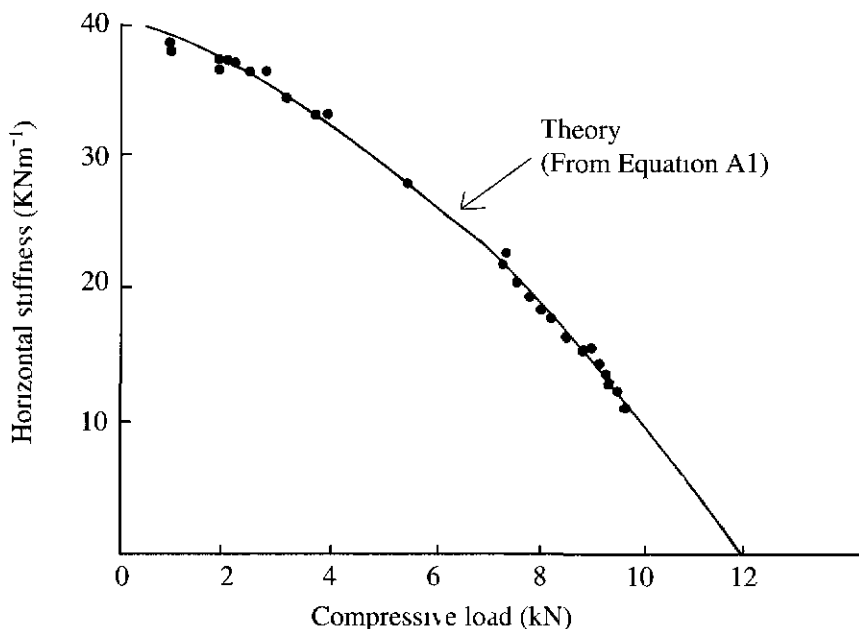


Figure 2 The horizontal stiffness of a model bearing as a function of compressive load. The full curve is based on Equation 4 with  $T$  (44 Nm<sup>2</sup>) and  $R$  (4.3 kN) values chosen to give the best fit.

Figure 3. The damping of the rubber out of which the bearings were made was found by an independent experiment in which the torsional damping of one of the bearings was measured under essentially zero compressive load. The effect of frequency on the damping of unfilled natural rubber was also investigated and found to be insignificant over the working range of 0.5 Hz to 5 Hz. Using Equation A7, the variation in damping of the bearings under horizontal oscillation can now be calculated using the parameters  $T$  and  $R$  determined earlier. The agreement between theory and experiment, as shown in Figure 3, is good. The magnitude of the change in damping with normal load is perhaps surprising, and indicates that the damping of a bearing may well be significantly greater than that of its constituent rubber when the safety factor is between 2 and 3 which may well be the case

in practice. The instability load of this bearing is 12.5 kN, thus for example a bearing operating at half the instability load (6.25 kN) will produce, from Figure 3, an increase in damping of some 80%.

The instability load (12.5 kN) for the bearing quoted above, was obtained by compressing a single bearing until it became unstable. It is interesting to compare this experimental value with the instability load predicted by Equations A4 and A5. For a bearing of overall height 98 mm, Equations A4 and A5 give instability loads of 11.9 kN, 13.9 kN respectively.

### Static Model Bearings

The experimental results of the height reduction of a model bearing with horizontal

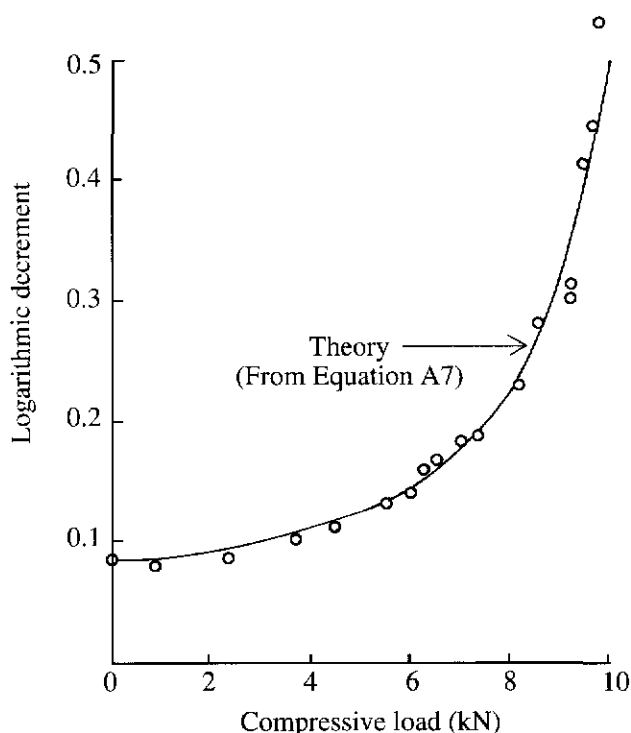


Figure 3. Variation in the logarithmic decrement of horizontal oscillations of a load supported by model bearings. The load per bearing is shown. The experimental points are corrected to 1 Hz and 13°C. The logarithmic decrement of a bearing under zero compressive load, found from separate torsional damping measurements, is 0.084.

displacement are shown in *Figure 4*, for compressive loads between 1 kN and 10 kN. The results were obtained using the quadruple shear apparatus described in this paper.

The height reduction can be seen to increase with increasing normal load. For modest shear displacements of 40% of the plan dimension of the bearing (*i.e.* 22 mm), in the direction of shear, the height reduction for the bearing operating at 2.5 kN normal load (a safety factor of 5) is some 0.56 mm or only 1.8% of the height of the rubber in the bearing. For contrast, at larger shear displacements for example 66% of the plan dimension (*i.e.* 36 mm) and 10 kN normal load (safety factor 1.25), the height reduction is 3.0 mm or 9.4% of the rubber height.

Such height reduction due to shearing, together with considerations of creep in the rubber under a normal load will determine clearance heights between a bearing and fail safe supports. A fail safe design is normally

provided in the event of a bearing undergoing extreme shear displacements due to an exceptionally severe earthquake.

The theoretical height reduction curves, derived from *Equation A6*, are also shown in *Figure 4*. The agreement between the experimental values and theory is found to be good, except where large displacements are applied to a bearing under a high compressive load. In this case, the theory is seen to progressively deviate from the experimental values, and predicts a slightly greater change in height than that found experimentally.

### Permissible Horizontal Displacement

In the event of a severe earthquake, a bearing may be required to undergo a horizontal displacement of perhaps as much as 200 mm or 300 mm. This is considerably greater than that usually required for applications such as bridge bearings which also have a similar rubber/metal laminate structure. An earth-

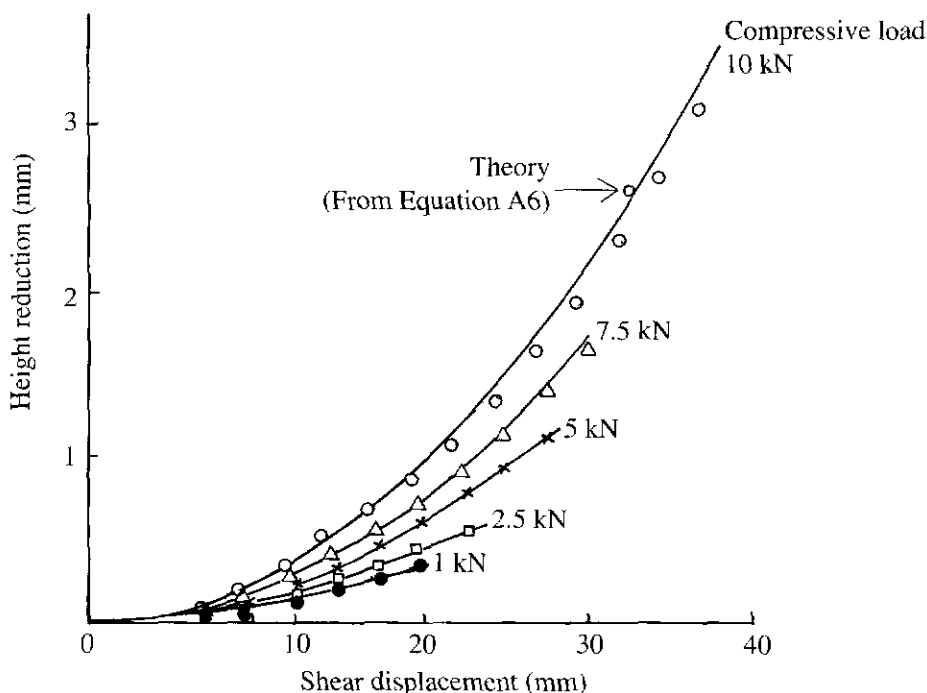


*Figure 4. The height reduction of a model bearing under shear with compressive loads between 1 kN and 10 kN.*

quake bearing will not, however, be required to undergo many horizontal deflections of this magnitude during its working life, probably no more than ten or twenty. Thus the usual rules giving the permissible deflections for bridge bearings are not relevant.

The behaviour of the model bearings, described earlier, under relatively large horizontal deflection with various compressive loads has been examined. *Figure 5* shows the nature of the deformation of a bearing under simultaneous compression and shear in the quadruple test apparatus. In practice, the steel reinforcing plates in a full-sized bearing are relatively thin and because of this some deformation of the plates could be expected, which makes analysis of the behaviour of the individual rubber layers difficult. In the case of the model bearings, the steel plates are made relatively thick so that deformation is negligible. Inspection of *Figure 5* indicates the general nature of deformation and it is seen that:

- A bending moment occurs which produces tilting in the individual layers.
- The greatest shear strain occurs at mid-height.
- Layer tilting causes tensile deformation at one end of the rubber layer and compression at the other.
- The degree of tension and compression is greatest at the end layers.

*Figure 6* shows the results of shear force *versus* shear displacement measurements on the model bearing described above.

Since the critical buckling load for the model bearings is about 12.5 kN, the normal loads reach values that are a much higher proportion of the buckling load than would be usual for full-sized bearings in practice. The shear force/deflection relation shows a reduction in stiffness with increasing normal load as expected theoretically (*Equation A1*).

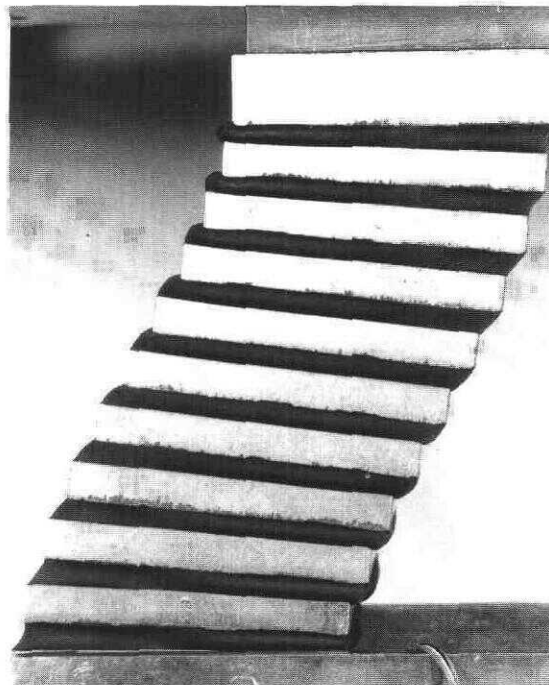


*Figure 5. A bearing under simultaneous compression and shear showing the different nature of the rubber deformation of individual layers.*

However, there is a maximum in the relation, showing that the linearity assumed in the theory breaks down at large enough horizontal displacements. The maximum occurs at a deflection which decreases with increasing normal load. For example, at 60% of critical load (7.25 kN) the maximum occurs at about 31 mm displacement or 58% of the bearings plan dimension (54 mm) in the direction of shear. As the critical load is approached, however, the corresponding shear displacement at maximum shear force reduces rapidly, thus for example at some 90% of critical load (11 kN) the maximum occurs at only 7 mm (13%) displacement. Since a bearing can only be expected to continue to support a structure while the shear force remains positive, the maximum shear displacement a bearing can sustain will occur just prior to zero shear force. For the bearing described here, supporting a compressive load of 10 kN, the maximum shear displacement is approximately 36 mm.

In practice, one would not normally allow a design in which the shear displacement exceeds that for maximum force because a greater displacement can produce permanent damage within the rubber, as discussed in the following section.

### Layer Tilting

The limiting shear displacement which a bearing can accept is not determined by the amount of shear which can be sustained by the individual rubber layers of the bearing. The maximum shear strain in the layers during the experiments of *Figure 6* is only about 100% which is well below the strain which could be sustained if the deformation were simple shear. A limitation occurs because the tilting of the layers seen in *Figure 5* introduces negative hydrostatic stresses which can lead to cavities or vacuoles forming in the rubber and subsequent crack propagation under sufficiently large stress conditions<sup>8</sup>.

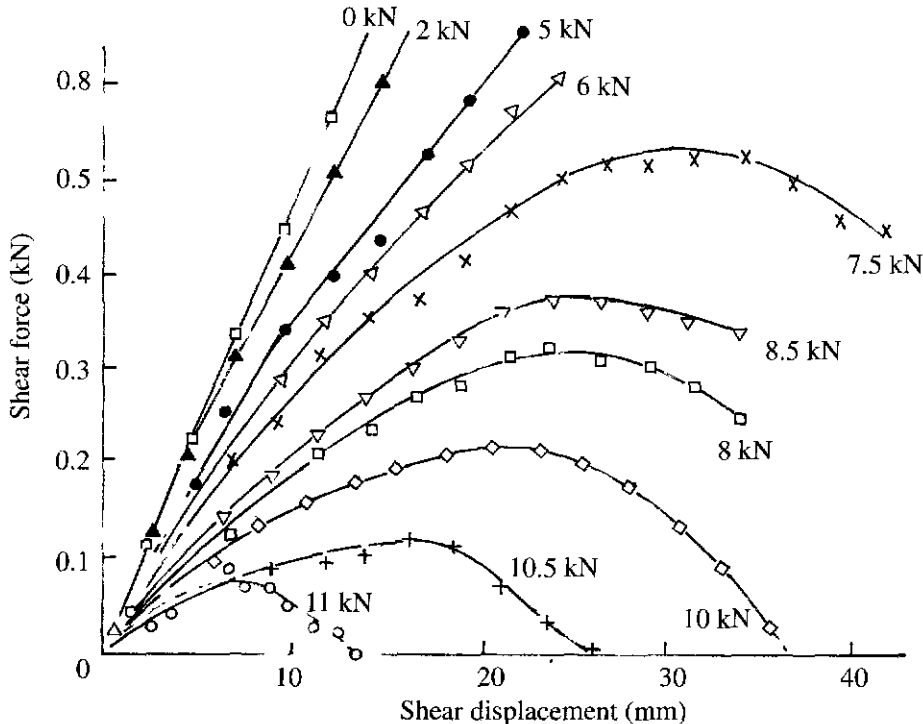


*Figure 6. The shear force versus shear displacement behaviour of a model bearing under various compressive loads.*



Since layer tilting is potentially a limiting factor in bearing performance this has been examined in more detail. Photographs of model bearings under simultaneous shear and compression, such as *Figure 5*, show clearly the angles of tilt of each successive rubber layer. It is possible from the photographs to measure the tilt angles and how these vary with overall shear strain and compression strain. The compressive and shear forces are measured so that it is possible to determine the bending moment which is being applied to each rubber layer.

*Figure 7* shows a force diagram for the bearing. The couple,  $C$ , at each end of the bearing is given by:

$$C = \frac{1}{2} (PY + Lt) \quad \dots 2$$

where

$P$  = compressive load

$L$  = shear load

$t$  = bearing height

$Y$  = shear displacement

At a bearing layer's mid-point  $(x, y)$  the bending moment  $B(x, y)$  is given by:

$$\begin{aligned} B(x, y) &= C - Py - Lx \\ &= \frac{1}{2} PY + \frac{1}{2} Lt - Py - Lx \\ &= P(Y/2 - y) + L(t/2 - x) \quad \dots 3 \end{aligned}$$

The bending moment in each layer of the bearing has been calculated using the equation above for three different overall shear dis-

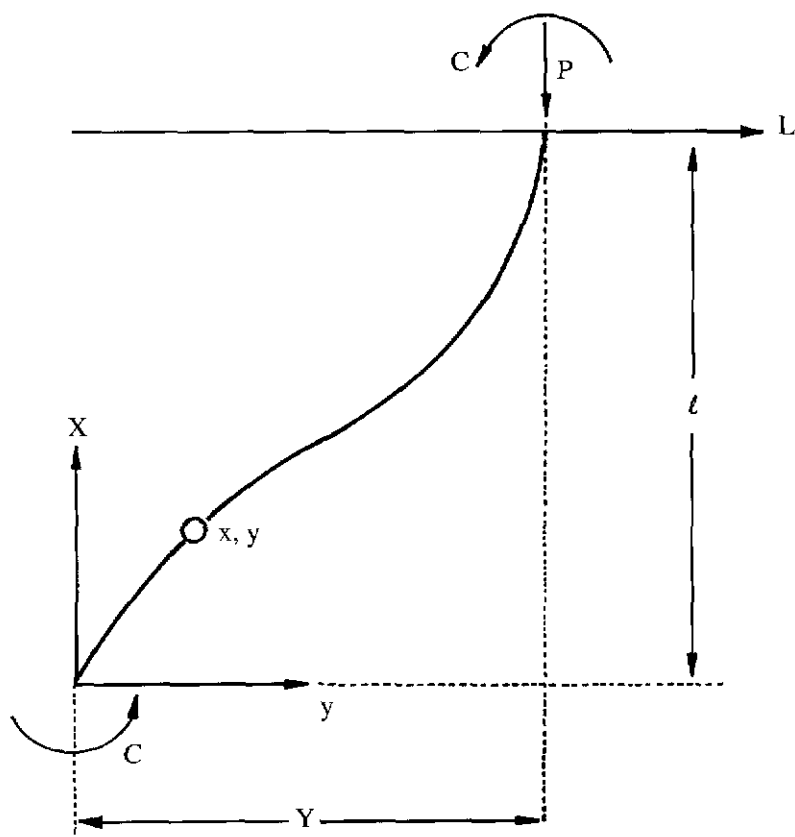


Figure 7. A force diagram for a bearing under combined compression and shear.

placements of the bearing, 24 mm, 38 mm, and 43 mm – corresponding to average overall shear strains in the rubber of 75%, 120%, and 135% respectively. *Figure 8* shows the relationship between these bending moments and the angles of tilt measured from the photographs. For a ‘well behaved’ rubber layer, the angle of tilt will be directly proportional to the bending moment and it is seen that this relationship is true for tilt angles of approximately one degree and less. From these measurements the value of  $T$ , the tilting stiffness, can be calculated from the constant of proportionality and gives a value of 43 kNm<sup>2</sup>, which agrees well with the value obtained from the free oscillation experiments described earlier in this paper. As the tilt angle becomes greater, however, *Figure 8* shows that the relationship becomes non-linear at bending moments above about  $1 \times 10^5$  N mm.

The source of the non-linearities shown in *Figure 6* can thus be traced to the corresponding non-linear behaviour in the bending moment/tilt angle relation for a single rubber/metal layer. At high bending moments the tilt increases rapidly. This effect will be most apparent in the rubber layers at the top and bottom of a bearing, such as that seen in *Figure 5*, where the bending moment is greatest. The probable cause of this decrease in tilting stiffness is the onset of cavitation in the rubber, producing vacuoles. Calculations show that the stresses are high enough to produce cavitation<sup>8</sup> and cavities have also now been detected visually.

As mentioned above the cavitation is due to the local hydrostatic tension produced by the tilting, and the vacuoles can be observed in model experiments using a transparent rubber.

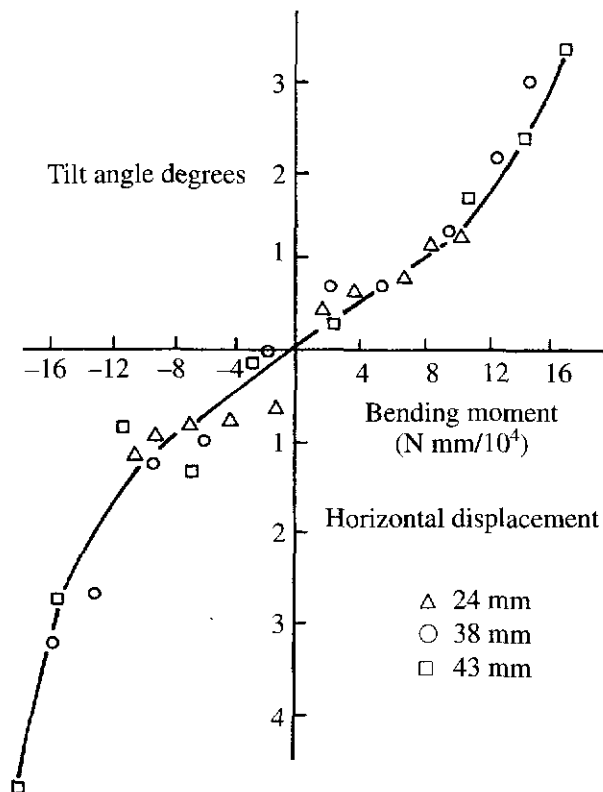


Figure 8. The relationship between bending moment and angle of tilt for rubber layers in a model bearing. Three different levels of shear displacement are shown.

Figure 9 shows the pressure distribution produced across a rubber layer by the compressive and tilting force components of a sheared rubber layer under a constant compressive load. A resultant negative hydrostatic pressure can be present in one half of a rubber layer when the negative tilting pressure component becomes greater than the positive pressure component provided by the compressive load on the bearing. When the negative hydrostatic pressure exceeds a critical value (approximately 0.8 of the Young's modulus of the rubber)<sup>8</sup> cavity formation will occur. Although the formation of vacuoles appears responsible for the reduction in shear stiffness of a bearing these vacuoles do not apparently propagate through the rubber layer in a destructive manner until significantly higher deflections than those at

which they are formed are reached. In the model experiments used to obtain the results in Figure 6 it is found that, provided strains corresponding to the force maximum have not been greatly exceeded, subsequent measurements show cavitation has had little effect on the overall stiffness of a bearing at small strains. This suggests that the cavities have produced only limited permanent damage, and merely close up on release of the load.

If the bearing is repeatedly subjected to strains in excess of the force maximum, cracks will propagate from cavity sites. An example of such crack propagation is shown in Figure 10 where a bearing is shown cut open after repeated cycling. The bearing has been repeatedly cycled thirty times to strains in excess of the force maximum and two cavities

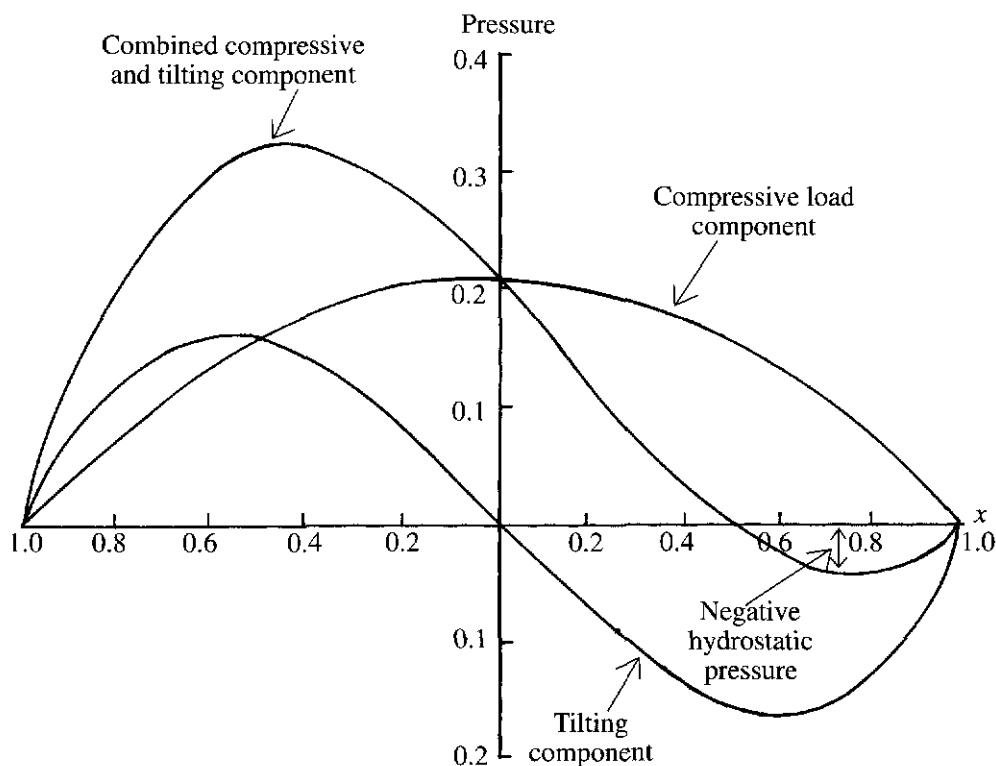


Figure 9. A pressure distribution diagram of a rubber layer in a bearing under combined compression and shear showing how a negative pressure may develop which can lead to internal failure. The units are non-dimensional.

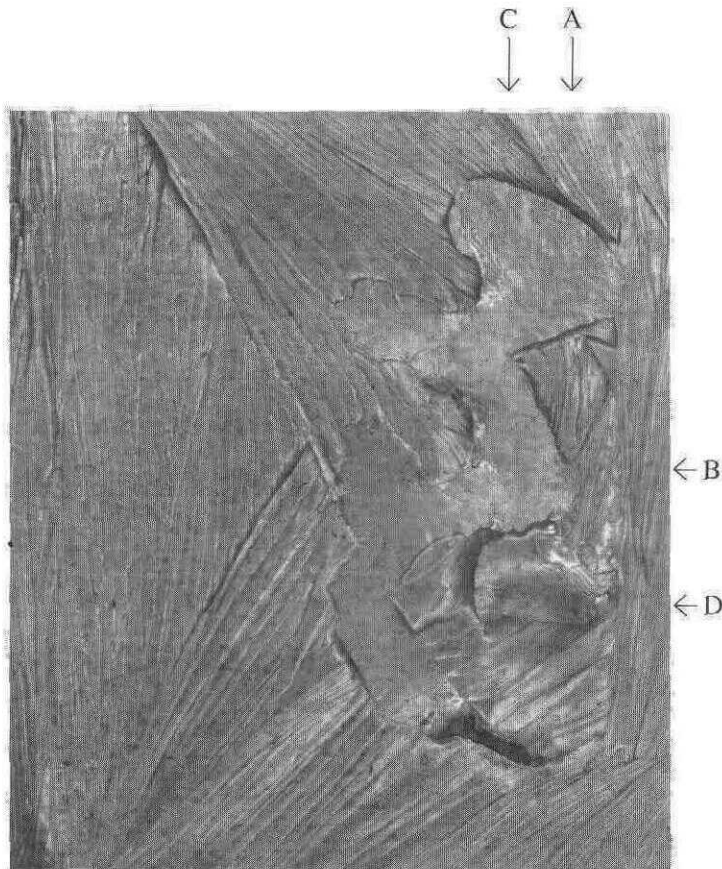


Figure 10. Photograph of a sectioned rubber layer subjected to repeated cycling (30 cycles) under combined compression and shear. Two crack propagation planes, caused by negative pressure, are shown on one half of the layer. The initial cavitation sites occurred at the intersect of AB and CD.



Figure 11. Photograph of a crack propagation plane, due to negative pressure, in a rubber layer of a bearing showing the crack surface contours in the form of concentric ridges. The initial cavity site can be seen at the intersect of AB.

are shown which have propagated to form the two failure planes. The initial cavity sites occur at the intersections of AB and CD. The major failure plane has propagated at approximately  $90^\circ$  to the normal compressive load while the minor failure plane is at a somewhat smaller angle (approximately  $70^\circ$ ). The cracks have propagated internally in the rubber throughout most of one half of the layer, the half in tension, in the areas of highest stress. Crack propagation is inhibited near the outer edge of the rubber, where the stress can be relieved, by deformation of the rubber at the free surface. *Figure 11* shows the major failure plane and initial cavity site in greater detail. Cracks have propagated from the cavity site forming a series of regular surface contours in the form of concentric rings.

#### CONCLUSIONS

The experimental work presented in this paper has successfully supported theory for the behaviour of important aspects of the mechanics of laminated rubber bearings. It has confirmed that the mechanical damping of a bearing can be considerably greater than that of the rubber itself with the application of a compressive load. Measurements of the height reduction of a bearing under shear, with a simultaneous constant compressive load, are found to agree well with the theory. Measurements of the dependence of shear stiffness of a bearing with compressive load have shown that shear stiffness reaches zero as the instability load is approached in the manner predicted. Studies of shear stiffness behaviour and the tilt angle of individual rubber layers at a known applied moment indicate a departure from the predicted linear behaviour which occurs at large deformations and suggests cavitation is responsible. It is confirmed that cavitation can occur by

examination of sectioned samples after testing. Initial cavity sites and subsequent crack propagation paths have been identified in the predicted region of a rubber layer. It is possible to operate a bearing in the non-linear shear region without catastrophic damage occurring, however, the onset of non-linearity may be considered a practical upper design limit for normal operation.

#### ACKNOWLEDGEMENTS

Thanks are due to Dr K. N. G. Fuller and Dr A.H. Muhr for comments on the manuscript.

*Date of receipt: October 1993*

*Date of acceptance: November 1993*

#### REFERENCES

1. THOMAS, A. G. (1982) The Design of Laminated Bearings I. *Proc. Int. Conf. on Natural Rubber for Earthquake Protection of Buildings and Vibration Isolation, Kuala Lumpur, Malaysia*, 229.
2. CHEMLOK 205/220. Rubber to Metal Bonding Adhesive supplied by Harcross Chemical Group, Durham Chemicals, Birtley, Chester-Le-Street, Co. Durham BH3 1QX, England.
3. HARINGX, J. A. (1948) *Philips Res. Rep.*, No. 6 and (1949); 4 no. 1 and 3.
4. GENT, A. N. (1964) Elastic Stability of Rubber Compression Springs. *J. Mech. Eng. Sci.*, **6**, 318.
5. PAN, T. C. AND KELLY, J. M. (1983) *Modal Coupling in Base-isolation Structures, Earthquake Engineering and Structural Dynamics II*, 749.
6. MALAYSIAN RUBBER PRODUCERS' RESEARCH ASSOCIATION (1980) Natural Rubber Engineering Data Sheets EDS 19.
7. GENT, A. N. AND MEINECKE, E. A. (1970) Compression, Bending and Shear of Bonded Rubber Blocks. *Polym. Eng. Sci.*, **10**, 48.
8. GENT, A. N. AND LINDLEY, P. B. (1958) Internal Rupture of Bonded Cylinders in Tension. *Proc. R. Soc. London*, **A249**, 195.

## APPENDIX

### Horizontal Stiffness of a Bearing

The theory for the horizontal stiffness  $k_s$  of a bearing was developed by Haringx<sup>3</sup> and applied to rubber laminated bearings by Gent<sup>4</sup> and is given by

$$k_s = \frac{P^2}{2qT \tan(q\ell/2) - P\ell} \quad \dots A1$$

$$\text{where } q^2 = \frac{P}{T} \left( \frac{P}{R} + 1 \right)$$

and  $T$  and  $R$  are the tilting and shear stiffness for unit height,  $\ell$  is the total height of the bearing, and the compressive load is  $P$ . The value of  $R$  is given by

$$R = GA \frac{t}{h} \quad \dots A2$$

where  $t$  is the total thickness of a column unit, consisting of a rubber layer and a rigid separating plate, and  $h$  is the thickness of a rubber layer.  $G$  is the shear modulus of the rubber.

For a circular cross section,

$$T = \frac{3G\pi r^4 t}{4h} \left( 1 + \frac{r^2}{6h^2} \right) \quad \dots A3$$

For other cross-sections, such as rectangles, the relation for  $T$  is rather more complicated but can still be evaluated<sup>4</sup>.

### Maximum Compressive Load on a Bearing

The maximum or critical compressive load  $P_c$  a bearing can sustain is given by

$$P_c = \frac{R}{2} \left[ \left( 1 + \frac{4\pi^2 T}{R\ell^2} \right)^{1/2} - 1 \right] \quad \dots A4$$

It is interesting to compare this relation to that given by the more conventional simple Euler strut theory. In this case, shear deformations are neglected and Equation A4 reduces to give

$$P_c = \frac{\pi}{\ell} \sqrt{TR} \quad \dots A5$$

### Height Reduction of a Bearing Under Shear

A simplification of the theory originally presented in Thomas<sup>1</sup> is given here. It describes the effect of height reduction of a bearing in shear under a constant compressive load.

The height reduction  $\Delta Z$  is given by

$$\frac{2qP^2}{F^2} \Delta Z = q\ell \left[ 1 + \frac{n}{2} (1+a^2) \right] - a(n+2) \quad \dots A6$$

where  $F$  is the shear force and  $n$  the number of rubber layers.

### Mechanical Damping of a Bearing

The mechanical damping of the bearing, expressed as the tangent of the loss angle, will be greater than that of the rubber from which it is made in the ratio  $D$  given by

$$D = \frac{(\text{Total work done on the rubber})}{(\text{Work done by the shearing force})}$$

$$D = \frac{\frac{q\ell n}{2} (1+a^2) - a}{a(n+1) - q\ell} \quad \dots A7$$

where  $n = 1 + 2P/R$

$$a = \tan \left( \frac{q\ell}{2} \right)$$